

# Interstellar Turbulence, Cloud Formation and Pressure Balance

Enrique Vázquez-Semadeni

*Instituto de Astronomía, UNAM, Apdo. Postal 70-264, México 04510, D.F., MEXICO*

**Abstract.** We discuss HD and MHD compressible turbulence as a cloud-forming and cloud-structuring mechanism in the ISM. Results from a numerical model of the turbulent ISM at large scales suggest that the phase-like appearance of the medium, the typical values of the densities and magnetic field strengths in the intercloud medium, as well as Larson’s velocity dispersion-size scaling relation in clouds may be understood as consequences of the interstellar turbulence. However, the density-size relation appears to only hold for the densest simulated clouds, there existing a large population of small, low-density clouds, which, on the other hand, are hardest to observe. We then discuss several tests and implications of a fully dynamical picture of interstellar clouds. The results imply that clouds are transient, constantly being formed, distorted and disrupted by the turbulent velocity field, with a fraction of these fluctuations undergoing gravitational collapse. Simulated line profiles and estimated cloud lifetimes are consistent with observational data. In this scenario, we suggest it is quite unlikely that quasi-hydrostatic structures on any scale can form, and that the near pressure balance between clouds and the intercloud medium is an incidental consequence of the density field driven by the turbulence and in the presence of appropriate cooling, rather than a driving or confining mechanism.

## 1. Introduction

One of the main features of turbulence is its multi-scale nature (e.g., Scalo 1987; Lesieur 1990). In particular, in the interstellar medium (ISM), relevant scale sizes span nearly 5 orders of magnitude, from the size of the largest complexes or “superclouds” ( $\sim 1$  kpc) to that of dense cores in molecular clouds (a few  $\times 0.01$  pc), with densities respectively ranging from  $\sim 0.1 \text{ cm}^{-3}$  to  $\gtrsim 10^6 \text{ cm}^{-3}$ . Moreover, in the diffuse gas itself, even smaller scales, down to sizes several  $\times 10^2$  km are active, although at small densities. Therefore, in a unified turbulent picture of the ISM, it is natural to expect that turbulence can intervene in the process of cloud formation (Hunter 1979; Hunter & Fleck 1982; Elmegreen 1993; Vázquez-Semadeni, Passot & Pouquet 1995, 1996) through modes larger than the clouds themselves, as well as in providing cloud support and determining the cloud properties, through modes smaller than the clouds (Chandrasekhar 1951; Bonazzola et al. 1987; Léorat et al. 1990; Vázquez-Semadeni & Gazol 1995). Moreover, another essential feature of turbulence is that all these scales

interact nonlinearly, so that coupling is expected to exist between the large-scale cloud-forming modes and the small-scale cloud properties.

In this chapter we adopt the above viewpoint as a framework for presenting some of the most relevant results we have learned from two-dimensional (2D) numerical simulations of the turbulent ISM in a unified and coherent fashion, as it relates to the problems of cloud formation, the phase-like structure of the ISM and the topology of the magnetic and density fields, as well as internal cloud properties, such as their virialization and scaling relations (§ 2.). Then, in § 3. we discuss further tests and implications of a fully dynamical picture of interstellar clouds and their sub-structure. § 3.1. discusses the correlation between the field variables, and the fact that fluid velocities are large at cloud boundaries in the simulations. § 3.2. discusses the feasibility of forming hydrostatic structures within a turbulent medium, and § 3.4. compares simulated line profiles and estimated cloud lifetimes with the corresponding observational data, showing there is good agreement. Then, § 3.5. discusses whether the results of the simulations can be considered applicable to molecular gas. Finally, § 4. presents a summary and some concluding remarks.

## 2. Cloud Formation and Properties in the Turbulent ISM

In a series of recent papers (Vázquez-Semadeni et al. 1995 (Paper I), 1996 (Paper III); Passot, Vázquez-Semadeni & Pouquet 1995 (Paper II)), we have presented two-dimensional (2D) numerical simulations of turbulence in the ISM on the Galactic plane, including self-gravity, magnetic fields, simple parametrizations of standard cooling functions for atomic and ionized gas (Dalgarno & McCray 1972; Raymond, Cox & Smith 1976) as fitted by Chiang & Bregman (1988), diffuse heating mimicking that of background UV radiation and cosmic rays, rotation, and a simple prescription for star formation (SF) which represents massive-star ionization heating by turning on a local source of heat wherever the density exceeds a threshold  $\rho_t$ . Supernovae are now being included (Gazol & Passot 1998; see also Korpi, this Conference, for analogous simulations in 3D). The simulations follow the evolution of a  $1 \text{ kpc}^2$  region of the ISM at the solar Galactocentric distance over  $\sim 10^8 \text{ yr}$  and are started with Gaussian fluctuations with random phases in all variables. The initial fluctuations in the velocity field produce shocks which trigger star formation which, in turn, feeds back on the turbulence, and a self-sustaining cycle is maintained. These simulations have been able to reproduce a number of important properties of the ISM, suggesting that the processes included are indeed relevant in the actual ISM. Some interesting predictions have also resulted.

### 2.1. Effective Polytrropic Behavior and Phase-Like Structure

One of the earliest results of the simulations is a consequence of the rapid thermal rates (Spitzer & Savedoff 1950), faster than the dynamical timescales by factors of  $10\text{--}10^4$  in the simulations (Paper I). Thus, the gas is essentially always in thermal equilibrium, except in star-forming regions, and an effective polytropic exponent  $\gamma_e$  (Elmegreen 1991) can be calculated, which results from the condition of equilibrium between cooling and diffuse heating, giving an effectively polytropic behavior  $P_{\text{eq}} \propto \rho^{\gamma_e}$ , where  $\rho$  is the gas density (see Papers

II and III for details).<sup>1</sup> Even though the heating and cooling functions used do not give a thermally unstable (e.g., Field, Goldsmith & Habing 1969; Balbus 1995) regime at the temperatures reached by the simulations, they manage to produce values of  $\gamma_e$  smaller than unity for temperatures in the range  $100 \text{ K} < T < 10^5 \text{ K}$ , implying that *denser regions are cooler*. Upon the production of turbulent density fluctuations, the flow reaches a temperature distribution similar to that resulting from isobaric thermal instabilities (Field et al. 1969), but without the need for them. Note, however, that in this case there are no sharp phase transitions. Furthermore, it is possible that the thermal instability does not have time to form structures in the presence of supersonic turbulence, since the isobaric mode of thermal instability in a region of size  $L$  condenses on characteristic timescale  $L/c$ , where  $c$  is the sound speed, while the turbulence shears the forming condensations on timescale  $L/v$ , where  $v > c$  is the characteristic turbulent speed at scale  $L$ . Work is in progress to decide on this issue.

## 2.2. Cloud Formation

In the simulations, the largest cloud complexes (several hundred pc) form simply by gravitational instability. Although in Paper I it was reported that no gravitationally bound structures were formed, this conclusion did not take into account the effective reduction of the Jeans length due to the small  $\gamma_e$  of the fluid. Once this effect is considered, it is found that the largest scales in the simulations are unstable. Nevertheless, inside such large-scale clouds, an extremely complicated morphology is seen in the higher-density material, as a consequence of the turbulence generated by the star formation activity. The medium- and small-scale clouds are thus turbulent density fluctuations (see also § 3.1.).

## 2.3. Cloud and magnetic field topology

The topology of the clouds formed as turbulent fluctuations in the simulations is extremely filamentary. This property apparently persists in 3D simulations (e.g., Padoan & Nordlund 1998). Interestingly, the magnetic field also exhibits a morphology indicative of significant distortion by the turbulent motions (Paper II; § 3.). The field has a tendency to be aligned with density features, as shown in fig. 1. Even in the presence of a uniform mean field, motions along the latter amplify the perpendicular fluctuations due to flux freezing, while at the same time they produce density fluctuations elongated perpendicular to the direction of compression. This mechanism also causes many of the density features to contain magnetic field reversals (e.g., the feature with coordinates  $x \sim 610$ ,  $y \sim 510$ ) and bendings (e.g., the feature at  $x \sim 700$ ,  $y \sim 550$ ). It happens also that magnetic fields can traverse the clouds without much perturbation, as seen for example in the feature at  $x = 630$ ,  $y = 600$ . These results are consistent with the observational result that the magnetic field does not seem to vary much along clouds (Goodman et al. 1990), and in general does not present a unique kind of alignment with the density features. On the other hand, recent observations

---

<sup>1</sup>Note that by “polytropic” here we only mean that an equation of “state” of the form  $P \propto \rho^{\gamma_e}$  is satisfied, with no implication whatsoever of equilibrium hydrostatic states, as is the case of equilibrium polytropes in stellar theory.

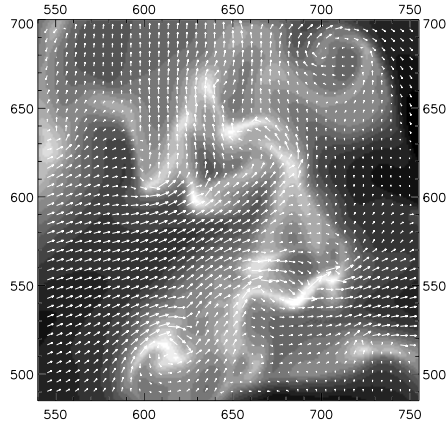


Figure 1. Gray-scale image of the logarithm of the density field, with superimposed magnetic field vectors. Shown is a subfield of  $250 \times 250$  pc ( $200 \times 200$  pixels), from a simulation at resolution of 800 grid points per dimension (VBR97). The minimum and maximum magnetic field intensities are  $0.12$  and  $20.1 \mu\text{G}$ , respectively. The axis labels show pixel number. See text for feature description.

have found field bendings and reversals similar to those described here (Heiles 1997).

It is important to note that the “pushing” of the turbulence on the magnetic field occurs for realistic values of the energy injection from stars and of the magnetic field strength, which ranges from  $\sim 5 \times 10^{-3} \mu\text{G}$  (occurring at the low density intercloud medium) to a maximum of  $\sim 25 \mu\text{G}$ , which occurs in one of the high density peaks, although with no unique  $\rho$ - $B$  correlation (Paper II). Thus, the simulations suggest that the effect of the magnetic field is not as strongly dominating as often assumed in the literature. This is also in agreement with the fact that the magnetic and kinetic energies in the simulations are in near global equipartition at all scales, as shown by their energy spectra (fig. 5 in Paper II), although strong local spatial fluctuations occur (Paper II; Padoan & Nordlund 1998).

Finally, note that the fact that the magnetic spectrum exhibits a clear self-similar (power-law) range, together with the fact that the fluctuating component of the field is in general comparable or larger than the uniform field, suggests strongly that the medium is in a state of fully developed MHD turbulence, rather than being a superposition of weakly nonlinear MHD waves.

#### 2.4. Cloud scaling properties

An important question concerning the clouds formed in the simulations is whether they reproduce some well-known observational scaling and statistical properties of interstellar clouds, most notably the so-called Larson’s relations between velocity dispersion  $\Delta v$ , mean density  $\rho$  and size  $R$  (Larson 1981), and the cloud mass spectra (e.g., Blitz 1991). Vázquez-Semadeni, Ballesteros-Paredes & Rodríguez (1997, hereafter VBR97) have studied the scaling properties of the clouds in the simulations, finding that the cloud ensemble exhibits a relation

$\Delta v \propto R^{0.4 \pm 0.08}$  and a cloud mass spectrum  $dN(M)/dM \propto M^{-1.44 \pm 0.1}$ , both being consistent with observational surveys, especially those specifically including gravitationally unbound objects (e.g., Falgarone, Puget & Pérault 1992). However, it was found that no density-size relation like that of Larson ( $\rho \propto R^{-1}$ ) is satisfied by the clouds in the simulations. Instead, the clouds occupy a triangular region in a  $\log \rho$ – $\log R$  diagram, as shown in fig. 8 of VBR97, with only its upper envelope being close to Larson’s relation. This implies the existence of clouds of very low column density, which can be easily missed by observational surveys if they do not integrate for long enough times. A few observational works, however, point towards the existence of transients (Loren 1989; Magnani, la Rosa & Shore 1993) and low-column density clouds, with masses much smaller than those estimated from virial equilibrium, and which exhibit a similar trend to that of the simulations, namely that of filling an area in a  $\log \rho$ – $R$  plot, bounded at large column densities by Larson’s density-size relation (Falgarone et al. 1992).

### 3. Tests and Implications of Clouds as Turbulent Density Fluctuations

One crucial implication of the interpretation that clouds are the turbulent density fluctuations in the ISM is that they are highly dynamical entities, a conclusion which conflicts with many models of cloud evolution based on equilibrium configurations, be it by external pressure confinement (e.g., Maloney 1988; Bertoldi & McKee 1992; McKee & Zweibel 1992, hereafter MZ92), or hydrostatic balance between (microscopic) internal MHD turbulence or wave support and self-gravity (e.g., Shu, Adams & Lizano 1987; Mouschovias 1987; Myers & Goodman 1988a,b), or combinations thereof (e.g., Zweibel 1990). It is thus important to turn to numerical simulations in which clouds form spontaneously, reproducing a number of observational cloud properties (§§ 2.4., 3.4.), and investigate their detailed density, velocity and magnetic fields in order to decide whether they are in a state of stationary equilibrium, and if not, whether a dynamical view is still consistent with available observational data.

In a recent paper (Ballesteros-Paredes, Vázquez-Semadeni & Scalo 1998, hereafter BVS98), we have started to perform work in this direction. In this section we will review some results from this work concerning the correlation between the density, velocity and magnetic fields, the evaluation of surface and volume kinetic terms in the Virial Theorem (VT), some comparisons with observational data, and then some implications, in particular whether it is feasible to expect the formation of hydrostatic structures within a turbulent medium.

#### 3.1. Correlation between variables, and kinetic Virial terms

In the scenario that clouds are turbulent density fluctuations, the essential concept is that they are *transient*, i.e., non-stationary. Note, however, that such transient character does not necessarily imply that the clouds will eventually disperse, since, under appropriate cooling (e.g., Hunter 1979; Hunter et al. 1986; Tohline, Bodenheimer & Christodoulou 1987; Paper III; § 3.2.) they can become gravitationally bound and collapse. Ballesteros-Paredes & Vázquez-Semadeni (1997) have indeed found in a sample of clouds that a small fraction of them

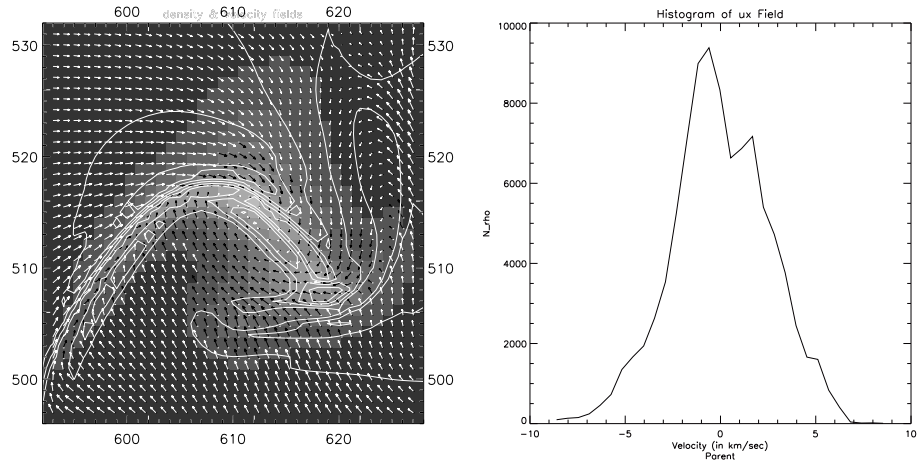


Figure 2. *a)* Enlargement of the feature at position  $x \sim 610$ ,  $y \sim 510$  in fig. 1, showing the logarithm of the density field (gray-scale), velocity field vectors (arrows, black for super-Alfvénic, white for sub-Alfvénic) and the magnitude of the magnetic field (contours, bolder indicating stronger fields). The cloud boundary is set at a density of  $8 \text{ cm}^{-3}$ . The maximum density within the cloud is  $55 \text{ cm}^{-3}$ . *b)* Density-weighted velocity histogram for the cloud in fig. 1. Note the multi-component structure.

has gravity strong enough to overwhelm the rest of the terms in the VT. In this scenario, then, clouds form at the collision sites of approaching gas streams, sites which can contain shocks if the motions are super-magnetosonic, and in which the highest densities (peaks) are located. We thus expect that, away from the density maxima, the velocity field be non-zero, and with a net convergence towards the peak.

Here it is necessary to note that cloud-defining algorithms are usually quite arbitrary in the way they define the cloud's extent, in the sense that they normally search for a density peak and then extend the cloud out to an arbitrary value, like the half-maximum (e.g., Williams, de Geus & Blitz 1994), or simply threshold the density at some arbitrary value and defining clouds as connected sets of pixels above the threshold (e.g., Ballesteros-Paredes & Vázquez-Semadeni 1997). In neither case are the outer boundaries of the clouds defined on any physical grounds. Observationally, molecular clouds are often claimed to have well-defined boundaries (e.g., Blitz 1991), but on the one hand this is likely an effect of the transition to atomic gas in the cloud periphery, and, on the other hand, there are counter-examples in which no sharp boundaries are observed (see BVS98 and references therein).

In view of the above, one expects that the velocity field should be non-zero when measured along arbitrarily-drawn cloud boundaries. Fig. 2a shows a magnification of the feature at position  $x \sim 610$ ,  $y \sim 510$  in fig. 2. This cloud spans roughly  $40 \times 30$  pixels in the simulation, (roughly  $50 \times 40$  pc). The gray-scale denotes the logarithm of the density; the arrows, the velocity field; and the contours, the magnetic field strength. The contours go from 4 to 10

$\mu\text{G}$  in intervals of  $1.5\mu\text{G}$ , with thicker contours denoting larger values of  $B$ . The black (white) arrows furthermore denote super- (sub-)Alfvénic velocities. Several points can be noticed. First, no velocity discontinuity is observed at the cloud boundaries, nor anywhere inside the cloud, except at its very center, where the velocity field vanishes. An oblique shock is seen to delineate the cloud “tail” on the left hand side of the figure. Significant vorticity is also seen around the cloud’s center. All of this is consistent with the cloud having been formed by a complex collision of turbulent streams.

An important consequence of the finiteness and continuity of the velocity field across the clouds’ boundaries is that it implies significant exchange of mass, momentum and energy through the boundary. This can be best evaluated by means of the kinetic terms in the Eulerian Virial Theorem (EVT; see, e.g., Parker 1979; MZ92), i.e., computed in an Eulerian frame, of fixed shape. Note, however, that we allow the Eulerian frame to move with the mean mass-weighted velocity of the cloud, in order to eliminate flux through the cloud’s boundary due to the cloud’s bulk motion. MZ92 have shown that, in its Eulerian form, the VT acquires a highly symmetrical form, in that the kinetic contribution to the VT is of the form  $\mathcal{E}_{\text{kin}} - \mathcal{T}_{\text{kin}}$ , where  $\mathcal{E}_{\text{kin}} = 1/2 \int_V \rho u^2 dV$  is a volume-integrated term giving the total kinetic energy in the cloud’s volume  $V$ , and  $\mathcal{T}_{\text{kin}} = 1/2 \oint_S x_i \rho u_i u_j \hat{n}_j dS$  is a surface integral over the cloud’s surface  $S$ . The latter term can be interpreted (BVS98) as the sum of the ram pressure plus the kinetic stresses dotted with the normal to the boundary, integrated over the boundary, in analogy with the corresponding terms for the thermal pressure and the divergence of the Maxwell stress tensor. Note, however, that, in contrast with the thermal pressure term,  $\mathcal{T}_{\text{kin}}$  contains non-isotropic contributions (BVS98). In the more familiar Lagrangian form of the VT (see, e.g., Shu 1992) the surface term does not appear, because the surface moves along with flow, implying zero flux across it.

BVS98 have calculated the two terms  $\mathcal{E}_{\text{kin}}$  and  $\mathcal{T}_{\text{kin}}$  for a sample of clouds in the simulation mentioned above, finding that in general both terms are comparable, evidencing the importance of the surface term compared with the total kinetic energy. Note that if both terms are equal, they cancel out, giving no net contribution to the VT, as is well known to be the case with the corresponding thermal pressure terms (e.g., Shu 1992). On the other hand, note that there are a few clouds for which  $\mathcal{T}_{\text{kin}}$  is negative, meaning that its contribution is of the same sign as that of  $\mathcal{E}_{\text{kin}}$ , towards an *expansion* of the cloud. More generally, the combined term  $\mathcal{E}_{\text{kin}} - \mathcal{T}_{\text{kin}}$  is in general nonzero, and of either sign, meaning it may contribute to compressions, expansions or generic distortions of the clouds.

### 3.2. Can hydrostatic structures form in a turbulent medium?

As mentioned above, a significant number of models of self-gravitating cloud cores have assumed that these structures are in (quasi-)hydrostatic equilibrium between self-gravity and some form of internal support, normally thought to be provided by a uniform field and Alfvén waves (e.g., Shu et al. 1987). However, a serious question is whether such hydrostatic configurations can be expected to form spontaneously in the turbulent environment in which they are known to dwell (turbulent molecular clouds). This problem has been addressed by BVS98 by considering the evolution of turbulently compressed polytropic masses of gas.

Note that in the following analysis, the internal pressure may be generalized to include sources of pressure other than thermal, such as magnetic or microturbulent. Note also that MHD wave pressure is expected to behave isotropically (Shu et al. 1987; McKee & Zweibel 1995).

It is well known (Chandrasekhar 1961) that in order for a collapsing spherical mass of gas to eventually stop and reach a hydrostatic equilibrium, it is necessary that  $\gamma_e > 4/3$ , so that the magnitude of the internal energy can increase faster than the gravitational energy during the collapse. This result has been generalized to collapse induced by compressions in  $n \leq 3$  dimensions (McKee et al. 1993; Paper III), finding that in this case the critical  $\gamma_e$  for collapse to be halted is  $\gamma_{cr} = 2(1 - 1/n)$ . If  $\gamma_e < \gamma_{cr}$ , the  $n$ -dimensional collapse cannot be halted. Conversely, if  $\gamma_e > \gamma_{cr}$  an initially gravitationally stable region cannot be rendered unstable by compression.

Therefore, BVS98 have pointed out that the formation of hydrostatic structures requires a *change* in  $\gamma_e$  during the collapse process. This is because, in order to start the collapse of an initially stable region by a turbulent compression,  $\gamma_e < \gamma_{cr}$  is required, but in order for internal pressure to later be able to halt the collapse, it is necessary that  $\gamma_e > \gamma_{cr}$ . Thus, unless  $\gamma_e$  changes during the collapse process, once the collapse is initiated it cannot be stopped by the internal pressure.

### 3.3. Implications for the Pressure of Interstellar Gas

The results described in § 3.1. have direct consequences on the underlying hypotheses of standard models of cloud confinement. Strictly speaking, clouds in the simulations are not “confined”, since they are transients. In other words, the left-hand side of the VT, the second time derivative of the cloud’s moment of inertia ( $\ddot{I}/2$ ), is in general nonzero (Ballesteros-Paredes & Vázquez-Semadeni 1997). In such a dynamical situation, clouds are *not* expected to be in thermal pressure balance with their surroundings, since the relevant driving mechanism is the *total* pressure, including thermal, kinetic and magnetic contributions (and cosmic rays, in the actual ISM). For example, the thermal pressure internal to a cloud may be increased due to the external ram pressure.

However, note that, because the atomic and ionized gas behaves as a polytrope with  $\gamma_e < 1$ , then the pressure difference between clouds and their surroundings is rather small. It is only when molecular densities are reached that  $\gamma_e$  becomes closer to (or possibly larger than) unity (Scalo et al. 1998), and higher thermal pressure contrasts between clouds and their environment are observed. In other words, in a turbulent medium in the presence of heating and cooling giving  $0 < \gamma_e < 1$ , the near constancy of the pressure is an incidental consequence of the combination of turbulent density fluctuation production and the low value of  $\gamma_e$ , rather than a controlling mechanism for cloud confinement. Conversely, note that, even if a cloud is in thermal pressure balance with its surroundings, this does not imply that it will be in a static equilibrium configuration, since ram pressure or simply inertial motions may distort a cloud.

Molecular clouds, on the other hand, are known to have much higher pressures, and traditionally this has been attributed to their being self-gravitating (e.g., Jura 1987). However, in the present scenario we expect there to also be



a significant contribution due to the conversion of external ram pressure into thermal pressure at  $\gamma_e \sim 1$ .

The possibility of cloud confinement by turbulent pressure has also been considered by MZ92. However, note that this mechanism implicitly assumes that the turbulence is microscopic, i.e., that the turbulent scales are much smaller than the size of the cloud. Otherwise, larger-scale modes imply the distortion of Lagrangian cloud boundaries (which move with the flow), or, equivalently, flux across fixed Eulerian boundaries.

### 3.4. Comparison with Observations

One crucial test for the dynamical scenario presented here is whether it compares favorably with observational data. In this section we discuss several lines of evidence that it does.

A first test is to obtain density-weighted velocity spectra, which can be compared with observational optically-thin line profiles. Figure 2b shows the density-weighted histogram of the  $x$ -component of the velocity ( $u_x$ ) for the cloud of fig. 1. This histogram may be compared with the  $^{13}\text{CO}$  line profile for the Rosette Molecular Cloud (RMC) shown in fig. 4 of Williams, Blitz & Stark (1995, hereafter WBS95).<sup>2</sup> Both clouds are comparable in many respects: while the RMC’s dimensions (as deduced from fig. 17 in WBS95) are  $\sim 90 \times 70$  pc, the simulated cloud is  $\sim 250 \times 120$  pc. Furthermore, the latter has a mean density of  $\sim 10 \text{ cm}^{-3}$ , while the gas sampled in the spectrum of fig. 4 of WBS95 has a mean density  $\sim 15 \text{ cm}^{-3}$ .

Comparing the histograms for both of these clouds, we note several points in common. First, both sets of data have FWHMs of roughly  $6 \text{ km s}^{-1}$  when only the main features are considered. Second, both sets exhibit high-velocity bumps, at several  $\text{km s}^{-1}$  from the centroid. Finally, and probably most importantly, the “main” features are seen to contain substructure in both sets of plots. However, while such features have been traditionally interpreted as “clumps”, in our simulations they originate from extended regions within the cloud.

A second comparison can be done at the level of the cloud lifetimes,  $\tau = L/\Delta v$ , where  $L$  is the cloud size and  $\Delta v$  its velocity dispersion. As an example, we calculate this for the cloud of fig. 2a. We find  $\Delta v = 2.3 \text{ km s}^{-1}$ , and  $l \sim 30$  pixels = 37.5 pc. Thus,  $\tau \sim 1.6 \times 10^7 \text{ yr}$ . This value is consistent with various estimates of GMC lifetimes of order a few  $\times 10^7 \text{ yr}$  (e.g., Bash, Green & Peters 1977; Blitz & Shu 1980; Larson 1981; Blitz 1994).

A third line of comparison concerns the topology of the density and magnetic fields. As discussed in § 2.3., the simulation results appear to be consistent with observations.

### 3.5. Applicability to molecular gas

The ISM simulations discussed in Paper II and BVS98 employ cooling functions which correspond to atomic and ionized gas, molecular cooling not being represented. Thus a natural concern is whether our results are applicable to

---

<sup>2</sup>Although fig. 4 in WBS95 shows  $^{12}\text{CO}$  spectra, which are optically thick, there is little, if any, qualitative difference with the optically thin  $^{13}\text{CO}$  spectra shown in fig. 5 of that paper.

molecular gas. Although the obvious ultimate test will be provided by simulations with appropriate molecular cooling, which will be presented elsewhere, there are strong reasons to believe the essential dynamical behavior will not be significantly modified. This is because the basic mechanism is the production of density fluctuations by turbulent compressive motions, which is independent of the “hardness” of the flow (determined by  $\gamma_e$ ). Instead, what appears to change with  $\gamma_e$  is the amplitude, profile, and statistical distribution of the density fluctuations (Passot & Vázquez-Semadeni 1998; Scalo et al. 1998), but the fluctuations themselves are necessarily produced by negative values of the velocity divergence for whatever value of  $\gamma_e$ . Therefore, all the results discussed above, which are a consequence of this density fluctuation production mechanism, are expected to be valid independently of the equation of state. In fact, simulations of isothermal compressible MHD turbulence (e.g., Padoan & Nordlund 1998; Ostriker et al. 1998; Mac Low et al. 1998), which may be thought of as using an equation of state more appropriate to molecular gas, necessarily exhibit turbulent density fluctuation formation as well.

The effect of self-gravity is likely to slow down the re-expansion of the denser structures, increasing the lifetime of structures that do not make it over the “internal energy barrier” and collapse, but again the principle that these are dynamical entities does not seem to be modified.

#### 4. Conclusions

In this paper we have reviewed the process of interstellar cloud formation by large-scale turbulence, and some of its consequences regarding the structure of the resulting clouds found in high-resolution 2D simulations of the turbulent ISM, such as the effective polytropic behavior, the topology and correlation of the density, velocity and magnetic fields, and the scaling relations that arise. Special attention was given to the implications of a dynamical conception of clouds, such as the important mass, energy and momentum fluxes across Eulerian (fixed) cloud boundaries, which equivalently imply severe distortions of Lagrangian (moving with the flow) boundaries.

We also discussed the implications on cloud pressure, which we suggested to be more an incidental consequence of the density field sculpted by the velocity field in the presence of specific heating and cooling laws determining the temperature and pressure, than a driving or confining agent for the clouds. This suggestion should be applicable at least for all structures in which thermal pressure is subdominant compared to turbulent and magnetic pressures, i.e., larger than a few tenths of a pc.

In this regard, we also discussed the applicability of the results, which are based on simulations that employ cooling functions appropriate for atomic and ionized gas, to molecular gas. We stressed that the basic mechanism of turbulent density fluctuation production is independent of the effective polytropic exponent. In fact, it is independent of dimensionality as well.

Finally, we discussed the possibility of forming hydrostatic structures within a turbulent environment in a polytropic fluid, as would be the case of quiescent molecular cloud cores. We suggested that this process would require that the effective polytropic exponent change during an ongoing collapse triggered by

the turbulence, a phenomenon which does not appear likely upon consideration of thermal, turbulent and magnetic wave pressures. Thus, we suggest that hydrostatic cores may not exist.

We wish to conclude, however, by noting that the dynamical scenario outlined here agrees in many respects with observations, as has been shown from velocity histograms, topology of the fields, cloud lifetimes estimates, scaling relations –except for a density-size relation–, etc. However, it does seem to differ significantly from stationary, equilibrium models of clouds.

**Acknowledgments.** I would like to thank Javier Ballesteros-Paredes and John Scalo for a careful reading of the manuscript and useful comments; J.B.-P. for extensive help with figure preparation, and the Conference organizers for their financial support and hospitality. The simulations were performed on the CRAY Y-MP 4/64 of DGSCA, UNAM. This work has received partial financial support from grants DGAPA/UNAM 105295 and CRAY/UNAM SC-008397.

## References

- Balbus, S. A. 1995, in *The Physics of the Interstellar Medium and Intergalactic Medium*, eds. A. Ferrara, C. F. McKee, C. Heiles & P. R. Shapiro (San Francisco: A.S.P.), p. 328
- Ballesteros-Paredes & Vázquez-Semadeni 1997, in *Star Formation, Near and Far*, ed. S. S. Holt & L. G. Mundy. (New York: AIP Press), p. 81
- Ballesteros-Paredes, Vázquez-Semadeni, & Scalo 1998, *ApJ*, in press (BVS98)
- Bash, F. N., Green, N., & Peters, W. L., III 1977, *ApJ*, 217, 464
- Bertoldi, F. & McKee, C. F. 199. *ApJ*, 395, 140
- Blitz, L. 1991, in *The Physics of Star Formation and Early Stellar Evolution*, eds. C. J. Lada & N. D. Kylafis (Dordrecht:Kluwer), p. 3
- Blitz, L. 1994, in *The Cold Universe*, eds. T. Montmerle, C. J. Lada, I. F. Mirabel, & J. Tran Than Van (Gif-sur-Yvette: Frontiers), p. 99
- Blitz, L., & Shu, F. H. 1980, *ApJ*, 238, 148
- Bonazzola, S., Falgarone, E., Heyvaerts, J., Péroult, M., & Puget, J. L. 1987, *A& A*, 172, 293
- Chandrasekhar, S. 1951, *Proc. R. Soc. London*, 210, 26
- Chandrasekhar, S. 1961, *Hydrodynamic and Hydromagnetic Stability* (Oxford: Clarendon)
- Chiang, W.-H., & Bregman, J. N. 1988, *ApJ*, 328, 427
- Dalgarno, A., McCray, R. A. 1972, *ARAA*, 10, 375
- Elmegreen, B. G. 1991, *ApJ*, 378, 139
- Elmegreen, B. G. 1993, *ApJ*, 419, L29
- Falgarone, E., Puget, J.-L., & Péroult, M. 1992, *A& A*, 257, 715
- Field, G. B., Goldsmith, D. W., & Habing, H. J. 1969, *ApJ*, 155, L149
- Gazol, A. & Passot, T. 1998, *ApJ*, submitted
- Goodman, A. A., Bastien, P., Menard, F. & Myers, P. C. 1990, *ApJ*, 359, 363
- Heiles, C. 1997, *ApJS*, 111, 245

- Hunter, J. H., Jr. 1979, *ApJ*, 233, 946
- Hunter, J. H. Jr., & Fleck, R. C. 1982, *ApJ*, 256, 505
- Hunter, J. H. Jr., Sandford, M. T. II, Whitaker, R. W. & Klein, R. I. 1986, *ApJ*, 305, 309
- Jura, M. 1987, in *Interstellar Processes*, eds. D. J. Hollenbach & H. A. Thronson (Dordrecht:Reidel), p. 3
- Larson, R. B., 1981, *MNRAS*, 194, 809
- Léorat, J., Passot, T., & Pouquet, A. 1990, *MNRAS*, 243, 293
- Lesieur, M. 1990, *Turbulence in Fluids*, 2<sup>nd</sup> ed. (Dordrecht:Kluwer)
- Lizano, S. & Shu, F. 1989, *ApJ*, 342, 834
- Loren, R. B. 1989, *ApJ*, 338, 902
- Mac Low, M.-M., Klessen, R. S. Burkert, & Smith, M. D. 1998, *Phys. Rev. Lett.*, 80, 2754
- Magnani, L., LaRosa, T. N., & Shore, S. N. 1993, *ApJ*, 402, 226
- Maloney, P. 1988, *ApJ*, 334, 761
- McKee, C. F. & Zweibel, E. G. 1992, *ApJ*, 399, 551 (MZ92)
- McKee, C. F., Zweibel, E. G., Goodman, A. A., & Heiles, C. 1993, in *Protostars and Planets III*, eds. E. H. Levy & J. I. Lunine (Tucson: U. Arizona Press), p. 327
- Myers, P. C. & Goodman, A. A. 1988a, *ApJ*, 326, L27
- Myers, P. C. & Goodman, A. A. 1988b, *ApJ*, 329, 392
- Padoan, P., Nordlund, A. 1998, *ApJ*, submitted
- Parker, E. N., 1979. *Cosmical Magnetic Fields. Their Origin and Their Activity* (Oxford: University Press)
- Passot, T., Vázquez-Semadeni, E., & Pouquet, A. 1995, *ApJ*, 455, 536 (Paper II)
- Passot, T. & Vázquez-Semadeni, E. 1998, *Phys. Rev. E*, in press (PVS98)
- Raymond, J. C., Cox, D. P., & Smith, B. W. 1976, *ApJ*, 204, 290
- Scalo, J. M. 1987, in *Interstellar Processes*, eds. D. J. Hollenbach & H. A. Thronson (Dordrecht:Reidel), p. 349
- Scalo, J., Vázquez-Semadeni, E., Chappel, D. & Passot, T., 1998, *ApJ*, 504, 835
- Shu, F. 1992, *Gas Dynamics* (Mill Valley: University Science Books)
- Shu, F. H., Adams, F. C., & Lizano, S. 1987, *ARAA*, 25, 23
- Spitzer, L., Savedoff, M. P. 1950, *ApJ*, 111, 593
- Vázquez-Semadeni, E., & Gazol, A. 1995, *A&A*, 303, 204
- Vázquez-Semadeni, E., Passot, T. & Pouquet, A. 1995, *ApJ*, 441, 702 (Paper I)
- Vázquez-Semadeni, E., Passot, T. & Pouquet, A. 1996, *ApJ*, 473, 881 (Paper III)
- Vázquez-Semadeni, Ballesteros-Paredes & Rodríguez, L. 1997, *ApJ*, 474, 292 (VBR97)
- Williams, J. P., de Geus, E. J., & Blitz, L. 1994, *ApJ*, 428, 693
- Zweibel, E. G. 1990, *ApJ*, 348, 186